Natural killer cells actively patrol peripheral lymph nodes forming stable conjugates to eliminate MHC-mismatched targets

Kym R. Garrod*, Sindy H. Wei*, Ian Parker*†, and Michael D. Cahalan*‡§

Departments of *Physiology and Biophysics and †Neurobiology and Behavior and ‡Center for Immunology, University of California, Irvine, CA 92697-4561

Edited by Philippa Marrack, National Jewish Medical and Research Center, Denver, CO, and approved May 14, 2007 (received for review March 27, 2007)

Natural killer (NK) cells are known to reject MHC-mismatched targets within blood organs, yet their role in peripheral lymphoid tissue remains unresolved. Here we address the capacity of NK cells to migrate within lymph nodes (LN) using two-photon microscopy to characterize cell velocities and interaction dynamics within the native lymphoid-tissue environment. Adoptively transferred unmanipulated NK cells were highly motile (6–7 μm/min) and capable of forming transient contacts with both syngeneic and allogeneic B cells. Stable conjugate interactions (lasting >5 min) formed preferentially with allogeneic cells, resulting in diminished motility and subsequent elimination of the target cell. In marked contrast to unmanipulated cells, NK cells purified by CD49b-positive selection exhibited only limited motility (2–3 μm/min). This velocity impairment arose largely because CD49b cross-linking enhanced NK cell adhesion to collagen fibers within the node. Moreover, CD49b cross-linking prevented NK cells from reconstituting effector cytolytic function *in vivo*, inhibited target cell lysis *in vitro*, and augmented IFN-γ responses to IL-2 activation *in vitro*. Taken together our data demonstrate that NK cells are a functionally important component of the LN microenvironment, and that cell motility and effector function are strongly modulated via CD49b manipulation.

motility | two-photon microscopy

Natural killer (NK) cells are a specialized subset of lymphocytes capable of mediating effector functions without the need for prior sensitization. To avoid aberrant autoimmune attack, NK cells express a diverse repertoire of inhibitory receptors that suppress lytic activity. Polymorphic Ly49 molecules specific for self-MHC class I constitute one of the best characterized family of inhibitory receptors (1). Under normal conditions, persistent engagement of Ly49 by cognate self-ligands results in recruitment of SHP-1 to the receptor's cytoplasmic immunoreceptor tyrosine-based inhibitory motif domain and subsequent dephosphorylation of activating signaling pathways (2). This inhibition of NK cell effector function is alleviated in the absence of self-molecules and is often the first step in acute rejection of allogeneic grafts. Although NK cell-mediated clearance of circulating MHC-mismatched targets is well established (3), the ability of NK cells to migrate to and eliminate allogeneic target cells from peripheral lymph nodes (LN) under homeostatic conditions remains poorly defined.

Recent evidence suggests that NK cells may exert important functional responses within LN. Specifically, enhanced recruitment of NK cells to antigen-stimulated LN facilitated the induction of a productive immune response (4). Moreover, Chen *et al.* (5) showed that LN NK cells efficiently lysed tumor cells and suppressed B16 melanoma metastasis to draining LN. These findings suggest that NK cells actively patrol the LN in search of cognate target and transformed cells, perhaps exhibiting robust motility similar to other lymphocyte subsets, such as T and B cells (6, 7). Therefore, it was surprising that NK cells isolated by DX5-positive selection were reported to move with slow velocity (2.75 $\pm$ 0.17 μm/min) when imaged in LN by two-photon microscopy (8).

DX5 is a monoclonal antibody commonly used to identify and isolate murine NK cells. DX5 binds the α_2-integrin CD49b (9). Integrins are heterodimers comprised of α- and β-subunits and are of key importance in several complex biological processes, including cell adhesion and migration (10). Experimental evidence indicates that integrin engagement can result in the activation of key signaling events (11). Specifically, cross-linking of β_1-integrins expressed on human NK cells transduces intracellular signals, leading to the activation of the Ras–MAPK cascade, subsequent IFN-γ production, and enhanced cytotoxicity (12). Therefore, CD49b cross-linking could induce signaling events that render positively selected NK cells immotile. To investigate this possibility, we used two-photon microscopy to visualize the *in situ* basal motility of unmanipulated NK cells within intact LN and examine their interaction dynamics with syngeneic and allogeneic B cells. Our results demonstrate that CD49b cross-linking strongly modulates motility, adhesion to collagen, and effector function, whereas unmanipulated NK cells are highly motile and preferentially form stable conjugates to eliminate MHC-mismatched target cells.

Results

NK Cells Home to LN, Localize to the T–B Boundary, and Are Highly Dynamic. To assess the capacity of NK cells to migrate to LN under homeostatic conditions, we adoptively transferred 5-(and-6)-carboxyfluorescein diacetate, succinimidyl ester (CFSE)-labeled $Rag^{-/-}$ splenocytes into wild-type (WT) recipients. $Rag^{-/-}$ donors lack T, B, and NK T cells (13), thereby allowing us to investigate homing and motility of NK cells without requiring positive selection procedures. FACS analysis of dissociated nodes showed >97% of the $CFSE^+$ cells were also $NK1.1^+$ and $CD122^+$, indicating that almost all of the labeled cells that had migrated to the LN were NK cells and not a contaminating population (Fig. 1*A*). Notably, the majority of the transferred cells were also $DX5^+$ (a pan-NK cell marker). Non-NK splenocytes presumably migrated to the lungs, liver, and spleen (14, 15) and were largely excluded from LN because of the lack of appropriate receptors required for high endothelial venule extravasation. Histological examination (Fig. 1*B*) of LN showed NK cells preferentially localized to the superficial cortex, concentrating near and adjacent to the edge of B cell

Author contributions: K.R.G. and M.D.C. designed research; K.R.G. performed research; S.H.W. and I.P. contributed new reagents/analytic tools; K.R.G. analyzed data; and K.R.G. wrote the paper.

The authors declare no conflict of interest.

This article is a PNAS Direct Submission.

Abbreviations: CFSE, 5-(and-6)-carboxyfluorescein diacetate, succinimidyl ester; LN, lymph nodes; KO, knockout; NK, natural killer.

§To whom correspondence should be addressed. E-mail: mcahalan@uci.edu.

This article contains supporting information online at www.pnas.org/cgi/content/full/0702867104/DC1.

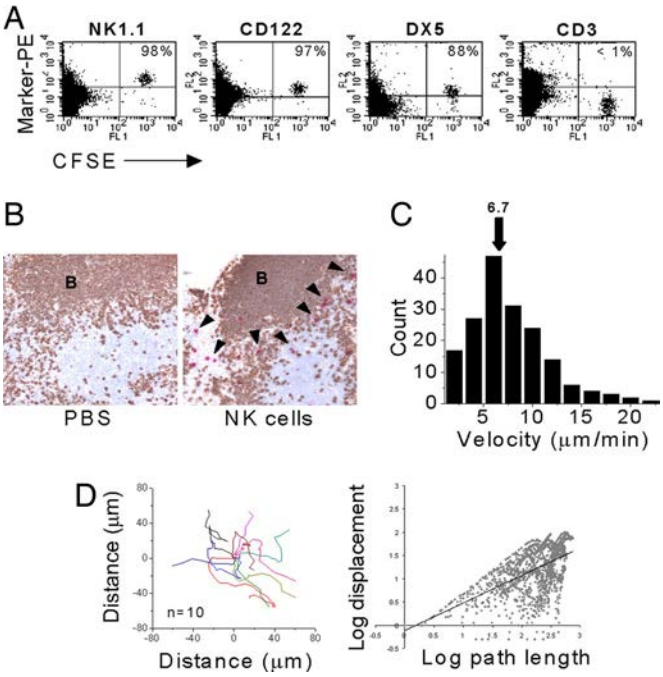

Fig. 1. NK cells home to LN, localize to the T–B boundary, and are highly motile. C57BL/6 Rag$^{-/-}$ splenocytes were stained with CFSE and adoptively transferred into C57BL/6 recipients. After 16–20 h, LN were harvested. (*A*) Two-color FACS dot plot of lymphocytes stained with PE-conjugated NK1.1, CD122, DX5, or CD3 Ab ($n = 4$). Numbers in upper right quadrants correspond to the percentage of CFSE-labeled cells (*x* axis) that expressed the indicated marker (*y* axis). (*B*) Frozen sections were stained to identify NK cells (red) and B cell (brown) zones. Micrographs depict LN from recipients receiving NK cells (*Right*) or PBS only (*Left*). Black arrowheads indicate individual NK cells. (Magnification: ×20.) (*C*) Distribution of mean velocities of individual NK cells within the LN (mean velocity = 6.7 ± 0.2 μm/min; $n = 176$ cells). (*D*) Trajectories of NK cells display random walk behavior. (*Left*) The *x-y* tracks of individual cells after normalizing to the same starting coordinate. (*Right*) A scatter plot of log displacement from origin versus log path length ($n = 1{,}549$ points). A regression line fitted to the log/log data has a slope of 0.5937, indicating that the mean displacement from origin increases in approximately direct proportion to the square root of total path length, as expected for a random walk process.

follicles. This pattern of NK cell localization within the LN is consistent with previous reports (8, 16).

To examine the behavior of unselected NK cells *in situ*, we used two-photon microscopy to study their mobility within lymphoid tissue. Individual NK cells exhibited robust motility [supporting information (SI) Movie 1] in a pattern of stop-and-go movement reminiscent of other lymphocyte subsets (6). Their mean velocity was 6.7 ± 0.2 μm/min (mean ± SEM), with some cells averaging as high as 20 μm/min (Fig. 1*C*). Within the regions of high NK cell density at the T–B boundary, individual NK cells followed apparently random, nondirectional paths (Fig. 1*D*). These results underscore the dynamic nature of NK cell motility and establish a minimally perturbed system to study NK cells in secondary lymphoid organs.

NK Cells Form Stable Conjugates to Eliminate MHC-Mismatched Targets. To investigate a functional role for NK cells in the peripheral lymphoid compartment, we examined NK–B cell interaction dynamics within regions of high NK cell density at the edge of B cell follicles in LN explants. In general, NK cells preferentially engaged in monogamous interactions, making transient contacts with both syngeneic and allogeneic B cells. The stability of these interactions was highly variable, ranging from 1 to >50 min, with the majority (>86%) of stable interactions (defined as lasting >5 min) occurring with allogeneic cells (Fig. 2*A* and SI Movie 2). Of note, we observed

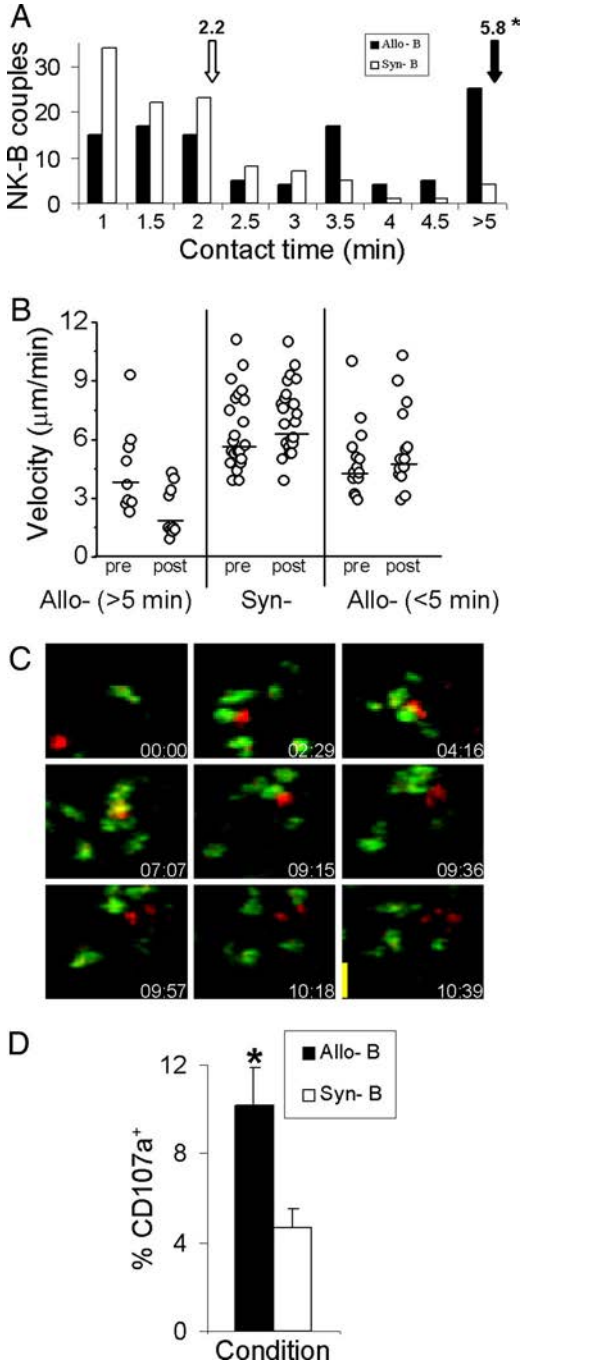

Fig. 2. NK cells form long-lasting contacts with MHC-mismatched B cell targets. NK cells were imaged in LN in the presence of either syngeneic B (syn-B) or allogeneic B (allo-B) cells. (*A*) Distribution of durations of NK–B cell interactions ($n = 150$, syn-B; $n = 145$, allo-B). Arrows indicate mean contact time (min) for syn-B (white) and allo-B (black) cells (*, $P < 0.001$, unpaired Student's *t* test). (*B*) Mean velocities of individual B cells were measured before (pre) and after (post) association with cognate NK cells. Data for syngeneic (*Center*) allo-B cells (contact time >5 min, *Left*; contact time <5 min, *Right*). Horizontal lines represent mean velocities for each condition. (*C*) Time-lapse images of an individual allo-B cell (red) engaging in a stable interaction with an NK cell (green). This association led to the recruitment of several NK cells (frame 07:07), resulting in elimination of the B cell target (frame 09:57). (Scale bar: 10 μm.) (*D*) C57BL/6 Rag$^{-/-}$ splenocytes were stained with CFSE and cotransferred with either syn-B (white bar) or allo-B (black bar) cells into C57BL/6 recipients. After 16–20 h, LN were harvested and CFSE^{+} cells were analyzed for lysosomal marker CD107a expression by FACS (*, $P < 0.05$). Results are representative of four independent experiments.

a pattern of NK cell behavior in which transient contacts usually preceded stable allogeneic interactions.

To determine whether LN NK cells were engaging in lytic interactions with allogeneic cells, we measured B cell velocities before and after association with cognate NK cells. It was previously established that reduced cell velocity of a target B cell is one of the earliest indicators of diminished cell viability (17). As demonstrated in Fig. 2*B*, syngeneic cell contacts, regardless of duration, resulted in no significant change in B cell velocity (pre- and postcontact motilities of 6.7 ± 0.4 and 7.3 ± 0.4 μm/min, respectively). For allogeneic cells, B cell velocities after contact with NK cells were also unaffected after short-duration interactions lasting <5 min (pre- and postcontact motilities of 5.0 ± 0.5 and 5.6 ± 0.6 μm/min, respectively). In contrast, stable allogeneic NK–B cell interactions lasting >5 min resulted in a 49% decrease in the velocity of the B cell target immediately after the encounter (pre- and postcontact motilities of 4.5 ± 0.8 and 2.3 ± 0.4 μm/min, respectively; $P = 0.01$). These results suggest that NK cells preferentially form stable conjugates to eliminate MHC-mismatched targets.

Interestingly, in some instances, stable conjugate formation with an allogeneic cell resulted in the recruitment of multiple NK cells swarming the B cell target. Immediately after these events, diminished motility of the allogeneic B cell target was rapidly accompanied by visible changes in cell morphology and membrane integrity, indicative of cytolysis (Fig. 2*C* and SI Movie 3). Up-regulation of CD107a (LAMP-1) on the cell surface has been shown to be a reliable marker for the identification of NK cell lytic effector function (18). Consistent with ongoing cytolytic activity of adoptively transferred LN NK cells, we found elevated levels of CD107a during the identical time frame when images were collected (Fig. 2*D*). Taken together these results demonstrate that NK cells actively patrol the LN in search of cognate target cells and support the idea that the lymphoid compartment is an important site for NK cell-mediated clearance of MHC-mismatched targets.

Positive Selection of NK Cells Inhibits *in Vivo* Motility. In contrast to our finding of vigorous NK cell motility, a recent report described NK cells as being relatively immotile in LN (mean velocity 2.75 ± 0.17 μm/min) (8). To reconcile these apparently conflicting results, we evaluated NK cell motility in the LN 20 h after different isolation procedures and *in vitro* treatments. Using the same commercially available isolation kit (MACS) as previously described (8), we found that positively selected $Rag^{-/-}$ splenic NK cells expressing CD49b ($DX5^+$) moved with lower velocities (3.4 ± 0.3 μm/min; SI Movie 4) than unselected NK cells from the same mice (6.8 ± 0.4 μm/min; Fig. 3*A*; $P < 0.0001$). A similarly reduced motility was observed by using a different DX5-positive selection kit (CELLection biotin binder; Dynal Biotech, Oslo, Norway) in which the beads were removed after isolation (data not shown). The reduced motility was not attributable to diminished viability because the NK cells did not exhibit a rounded-up morphology characteristic of dead or dying cells, but rather displayed dynamic behavior, frequently extending and retracting projections (SI Movie 5).

By direct examination of cotransferred cells, we next compared the motility of unmanipulated NK cells with NK cells exposed to DX5 microbeads, but not purified through a column (Fig. 3*A*), and with cells subjected to DX5 cross-linking (Fig. 3*B*). Imaged side by side in the same recipients, we again found unmanipulated NK cells to be highly motile, in contrast to NK cells after treatment with DX5 microbeads (3.6 ± 0.2 μm/min; SI Movie 6; $P < 0.0001$). A similarly slow motility (3.3 ± 0.3 μm/min) was observed after DX5 cross-linking, whereas cotransferred isotype control cross-linked cells imaged simultaneously moved vigorously (6.0 ± 0.3 μm/min; $P < 0.0001$). Importantly, NK cells that were treated with DX5 Ab, but without cross-linking (6.1 ± 0.4 μm/min), moved with velocities comparable to unmanipulated NK cells. These results demonstrate that NK cells display robust motility in secondary lymphoid organs under physiological conditions and indicate that positive selection procedures inhibit NK cell mobility via CD49b cross-linking.

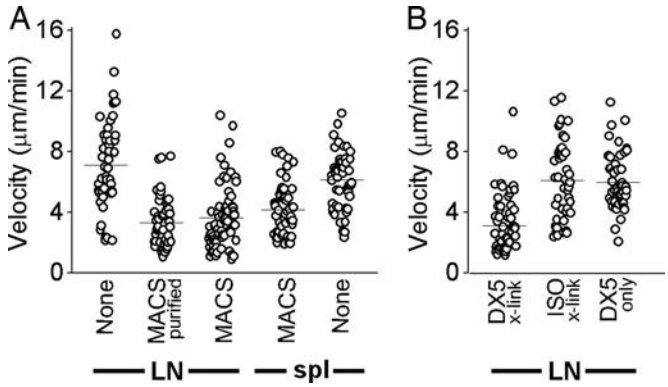

Fig. 3. DX5-positive selection inhibits NK cell motility. Mean velocities of adoptively transferred NK cells that were left untreated (none), DX5-positively selected (MACS-purified), exposed to DX5 microbeads but not purified through a column (MACS) (*A*), or treated with CD49b-biotin (DX5) or rat IgM-biotin isotype control (ISO), followed by the addition of streptavidin (x-link) or PBS (DX5 only) (*B*). Velocities were calculated from two-photon imaging of spleen (spl; *A*) and LN (*A* and *B*). Horizontal lines represent mean values for each condition.

We also imaged NK cells in the spleen and found no significant differences between the LN and splenic compartments for the velocities of each group of NK cells (Fig. 3*A*). Once again, CD49b cross-linking reduced the motility of NK cells imaged within the spleen. Thus, the diminished NK cell motility in the LN after CD49b cross-linking does not arise because a subset of NK cells that migrate at high velocities fail to home to the node.

CD49b Cross-Linking Enhances NK Cell Adhesion. CD49b (α_2) heterodimerizes with CD29 (β_1) to form the integrin receptor VLA-2 ($\alpha_2\beta_1$) (19). The principal ligand for VLA-2 is collagen (20). Because the LN architecture includes a collagen fiber network, the observed decrease in NK cell motility after positive selection could be because of an inability to adhere to or dissociate from collagen, either of which may inhibit NK cell migration along the collagenous matrix within the LN. We thus performed *in vitro* assays to assess NK cell adhesion to collagen after CD49b cross-linking. Treatment of $Rag^{-/-}$ splenocytes with DX5 microbeads resulted in an ≈50% increase in the fraction of cells that adhered strongly to a collagen substrate (Fig. 4*A Left*). Similar results were obtained by using cells treated with DX5 Ab plus streptavidin, whereas isotype control cross-linking did not alter the basal adhesion of the cells. To confirm that this effect was specific to NK cells, we sorted $NK1.1^+$ WT splenocytes and consistently found enhanced NK cell adhesion to collagen-coated plates *in vitro* after the same CD49b cross-linking that suppresses motility in the LN (Fig. 4*A Right*).

To evaluate further the consequences of the enhanced adhesion on NK cell behavior *in vivo*, we adoptively transferred CD49b cross-linked NK cells into WT recipients to examine the interaction of NK cells with collagen fibers in the LN. By direct observation of 39 treated NK cells that were covisualized making contact with collagen fibers, we found that a majority of these cross-linked cells (30 of 39) were immotile. Interestingly, when the rare motile CD49b cross-linked NK cells, exhibiting an instantaneous velocity of 6.1 ± 0.5 μm/min, encountered a fiber,

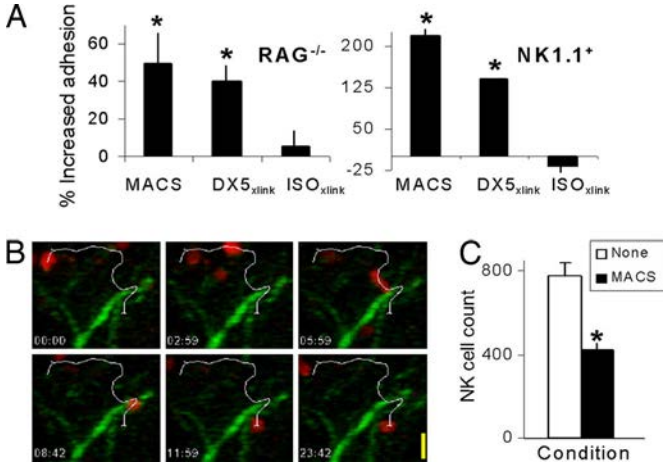

Fig. 4. CD49b cross-linking enhances NK cell adhesion and reduces homing to LN. (*A*) $Rag^{-/-}$ splenic (*Left*) or WT NK1.1$^+$ sorted (*Right*) NK cells were treated as indicated. After incubation on collagen I-coated plates for 1 h at 37°C, the numbers of adherent cells were determined and are expressed as a percentage of untreated control values. Data are representative of three independent experiments. (*B*) Time-lapse images illustrate a CD49b cross-linked NK cell (red) that encountered a collagen fiber (green) within the LN and subsequently remained trapped for the remaining period of imaging (>10 min). White overlay shows the track of the NK cell throughout the entire duration of the recording. Imaging depth was 27.5 μm below the LN capsule. (Scale bar: 10 μm.) (*C*) $Rag^{-/-}$ splenocytes were CFSE-labeled, split into two aliquots, and either treated with DX5 microbeads (MACS) or left untreated (none). Equal numbers of cells were injected into WT recipients. Sixteen to 20 h after adoptive transfer, LN were harvested, stained with NK1.1 Ab, and analyzed by FACS. To compare homing efficiency between samples, NK cell (CFSE$^+$/NK1.1$^+$) counts were calculated by using an equal number of FS/SS-gated events ($n = 3$ recipients per condition) (*, $P < 0.005$).

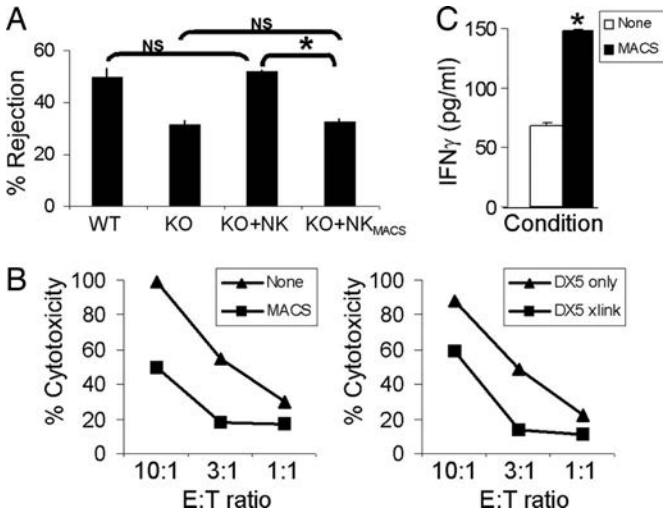

Fig. 5. CD49b cross-linking alters NK cell effector function. (*A*) Equal numbers of syngeneic and allogeneic B cells were transferred into WT recipients, $\gamma c^{-/-}$ recipients (KO), or KO recipients reconstituted with exogenous unmanipulated (KO + NK) or DX5 microbead-treated NK cells (KO + NK_{MACS}). The following day, spleens were harvested, and the percentage of syngeneic/allogeneic cells remaining after 12–16 h was determined by FACS analysis ($n =$ 3 mice per group). (*B* and *C*) $Rag^{-/-}$ splenic NK cells were treated as indicated and subsequently cultured in the presence of IL-2: untreated (filled triangle, none), DX5-microbeads (filled square, MACS), CD49b-biotin Ab (filled triangle, DX5 only), or CD49b-biotin Ab plus streptavidin (filled square, DX5 x-link). After 2 days, NK cells were used for *in vitro* cytotoxicity assays (*B*), and IFN-γ concentration in the supernatant was determined (*C*) ($n = 3$). Percent rejection was calculated as described in *Materials and Methods*. *, $P < 0.05$; NS, not statistically significant.

they usually attached and stopped moving (Fig. 4*B* and SI Movie 7). This behavior was in contrast to unmanipulated NK cells, which remained motile after contact and migrated along collagen fibers (31 of 33 cells; SI Movie 8). We next determined the velocities of CD49b treated and unmanipulated NK cells visualized as contacting collagen fibers and found their average instantaneous velocities to be 2.9 ± 0.2 and 7.4 ± 0.3 μm/min, respectively. Therefore, the mechanism of diminished *in vivo* motility of positively selected NK cells is largely attributable to their propensity to irreversibly adhere to collagen fibers within the LN.

In light of these findings, we investigated whether CD49b cross-linking of NK cells before adoptive transfer could result in diminished migration to LN due to CD49b-induced adhesion to peripheral tissue. Consistent with this interpretation, we recovered significantly fewer cross-linked NK cells from LN when compared with unmanipulated controls (Fig. 4*C*), further highlighting potential complications of using DX5-positive selection to purify NK cells.

CD49b Cross-Linking Skews NK Cell Effector Function. To explore a possible functional consequence of CD49b cross-linking, we compared the effector function of unmanipulated NK cells to that of NK cells treated with DX5 microbeads. We first established the assay conditions by measuring the abilities of WT mice and common γ-chain-deficient [knockout (KO)] mice that lack mature NK cells to eliminate MHC-mismatched cells by cotransferring syngeneic and allogeneic B cell targets into each recipient. As expected, the WT mice rejected a majority of allogeneic cells, whereas the KO recipients were unable to efficiently clear the target cells (Fig. 5*A*). To determine whether CD49b cross-linking alters NK cell cytolytic function, we reconstituted the KO mice with exogenous untreated or DX5 microbead-treated NK cells. The KO mice reconstituted with untreated NK cells were equally efficient in rejecting allogeneic cells as WT recipients, whereas those reconstituted with CD49b cross-linked NK cells showed diminished target cell clearance at levels comparable to KO recipients (Fig. 5*A*). Consistent with these *in vivo* results, we also found that CD49b cross-linking limited the ability of NK cells to kill MHC-mismatched targets *in vitro* (Fig. 5*B*). To assess the role of CD49b manipulation on cytokine production by NK cells, we examined IFN-γ levels under IL-2-activating conditions. Notably, IFN-γ production more than doubled after CD49b cross-linking (Fig. 5*C*). Taken together our findings reveal numerous consequences of positive selection on NK cell function and thus compel a reexamination of previous research employing DX5-positive selection.

Discussion

This study clearly establishes that NK cells exhibit remarkably dynamic behavior in secondary lymphoid tissue. We demonstrate that NK cells preferentially localize to the edge of B cell follicles, thereby facilitating interactions and subsequent elimination of MHC-mismatched B cells. Such surveillance may also play a role in preventing spontaneous B cell lymphomas that occur in NK cell-deficient animals (21). Moreover, we demonstrate that motility and effector function can be modulated via CD49b manipulation.

Using two-photon microscopy, we note several striking similarities in NK cell behavior to that of other lymphocyte subsets previously imaged in peripheral LN. First, NK cells move in an ameboid, stop-and-go manner along meandering paths, displaying average velocities comparable to B cells (6). Second, we show that, similar to T and B cells, NK cells occupy a distinct niche within the LN compartment. Specifically, NK cells localized to

regions overlapping the T and B cell zones at the T–B boundary. Third, NK cells were observed actively patrolling their microenvironment, forming cell–cell contacts to sample syngeneic as well as allogeneic B cells. Mempel *et al.* (17) recently provided a detailed analysis of cytotoxic T cell-mediated clearance of cognate B cell targets in which antigen recognition triggered immediate stable conjugate formation, resulting in irreversible arrest and death of the target B cell. We also observed diminished B cell motility as an early sign of cell lysis after stable contacts with NK cells. In contrast to the strictly monogamous CTL–B cell interactions (17), NK cells were occasionally seen swarming a target, leading to its destruction (SI Movie 3). Last, as demonstrated for other lymphocytes (22, 23), our results validate the feasibility of immunoimaging approaches to investigate the participation of NK cells in shaping immune responses within the native lymphoid-tissue environment.

Our results indicate that the limited NK cell mobility previously reported (8) is an artifact of cell isolation procedures and does not accurately reflect intrinsic NK cell behavior. Impaired NK cell motility is a direct result of CD49b-induced adhesion of positively selected NK cells to collagen fibers within the node. The effect of CD49b cross-linking on motility is remarkably long-lasting, inhibiting motility in the LN at least 20 h later. In line with our findings, previous work has shown that receptor cross-linking can regulate leukocyte function. Specifically, Fanning *et al.* (24) found that positive selection procedures using a magnetic bead cell isolation kit to obtain pure populations of plasmacytoid dendritic cells led to the inhibition of IFN-α production in response to viral stimulation. Together these results highlight the importance of appropriate cell preparation techniques for replicating physiological conditions.

Furthermore, we uncovered a potentially important function for CD49b, in which receptor cross-linking skews NK cell effector function to a phenotype that exhibits a high level of IFN-γ production along with a concomitant reduction in motility and cytolytic activity. Emerging evidence demonstrates that human NK cells can differentiate into immunoregulatory ($CD56^{bright}$) and cytolytic effector ($CD56^{dim}$) subsets depending on the environmental milieu (16, 25). Thus, similar to the human NK cell dichotomy, our data suggest that murine NK cell effector function could equally segregate into two distinct subsets: cytokine-producing helper cells (NK_h) and cytolytic effector cells (NK_c). We propose that CD49b cross-linking may mimic the *in vivo* effects of a collagen-rich environment, in which NK cells recruited to sites of inflammation, such as the skin, can provide help to resident antigen-presenting cells by secreting IFN-γ. This suggestion is supported by evidence demonstrating that, in an experimental mouse model of psoriasis (26), immunocytes isolated from skin lesions displayed classic NK cell markers, a scenario reminiscent of human immunoregulatory ($CD56^{bright}$) NK cells that accumulate in psoriatic skin (27). Therefore, the tissue composition to which NK cells are recruited may skew NK cell effector function, suggesting yet another level of control over lymphocyte effector fate. Further studies that can recapitulate the effects of CD49b cross-linking *in vivo* are required to elucidate the exact role of CD49b engagement under physiological conditions.

In summary, our results show that NK cells actively patrol the lymph node and preferentially form stable conjugates to eliminate MHC-mismatched target cells. This report shows robust NK cell motility *in vivo* and reduction in NK cell velocity by CD49b engagement during positive selection. In addition, our study provides a system to study NK cells in peripheral lymphoid tissue. With NK cells emerging as one of the key players in bridging innate and adaptive immune responses (28–30), it will be of interest to examine the NK–DC–T cell interplay by using real-time imaging techniques.

Materials and Methods

Animals. Female 5- to 10-week-old C57BL/6, BALB/c, B6.129S7-*Rag1*^{tm1Mom}/J ($Rag^{-/-}$), and B6.129S4-*Il2rg*^{tm1Wjl}/J ($\gamma c^{-/-}$) mice were purchased from The Jackson Laboratory (Bar Harbor, ME). Rag deficiency was confirmed through FACS analysis by the absence of contaminating T and B cells and/or macroscopic examination of the spleen (microsplenia). Mice were housed in a pathogen-free animal facility, and all procedures were performed in accordance with protocols approved by the Animal Care and Use Committee of University of California, Irvine.

Antibodies and Other Reagents. PE-labeled monoclonal antibodies [CD49b (clone DX5), NK1.1, CD122, CD3], DX5-biotin, CD107a-pure, Fc block (anti-CD16/CD32), and isotype controls were purchased from eBioscience (San Diego, CA). Anti-rat IgG-PE (Jackson ImmunoResearch Laboratories, West Grove, PA) was used to detect CD107a expression. A DX5-positive selection kit was purchased from Miltenyi Biotec (Auburn, CA). CFSE, 5-(and-6)-(((4-chloromethyl)benzoyl)amino)tetramethylrhodamine, and 7-amino-4-chloromethylcoumarin were purchased from Molecular Probes (Eugene, OR).

Adoptive Transfer Experiments. RBC-lysed splenocytes (30–40% $NK1.1^+$) from C57BL/6 $Rag^{-/-}$ donors were the source of NK cells for all experiments unless otherwise indicated. For CD49b cross-linking experiments, NK cells were treated with 10 to 20 μl/10^6 cells DX5 microbeads (MACS; Miltenyi Biotec) or 5 to 10 μg/10^6 cells DX5-biotin Ab for 20 min on ice, followed by 100 μg/10^6 cells streptavidin. Then 5 to 10×10^6 B cells and/or 1 to 1.5×10^7 NK cells were injected i.v. into C57BL/6 recipients.

Immunohistochemistry. LN from recipients were harvested 16 to 20 h after adoptive transfer of CFSE-labeled NK cells. Frozen sections were stained with anti-FITC-alkaline phosphatase and anti-mouse IgD and detected by using Fast-Red and anti-Rat IgG-horseradish peroxidase. Peroxidase activity was developed by using diaminobenizidine, and tissue was counterstained in hematoxylin.

Two-Photon Imaging and Analysis. Sixteen to 20 h after adoptive transfer of cells, spleen and LN (axillary, brachial, and inguinal) were harvested, secured with cyanoacrylate adhesive onto a coverslip (with the cortical region of the LN facing the objective), and placed in an imaging chamber superfused with RPMI medium bubbled with carbogen (95% O_2/5% CO_2) at 37°C. Two-photon imaging was performed as previously described (6). In brief, multidimensional imaging was performed with femtosecond-pulsed excitation at 780 nm. To detect CFSE-, 5-(and-6)-(((4-chloromethyl)benzoyl)amino)tetramethylrhodamine-, and 7-amino-4-chloromethylcoumarin-labeled cells, dichroic mirrors (560 and 510 nm, respectively) were used to split fluorescence emission into three photomultiplier detector channels. Collagen fibers were covisualized by detection of backscattered second harmonic generation employing femtosecond excitation at 780 nm and detection using a 390/70 bandpass filter. Unless otherwise indicated, successive imaging volumes immediately beneath the capsule were acquired at 18- to 21-sec intervals. Images were acquired, processed, and analyzed by using MetaMorph software. Imaris Bitplane software was used to visualize NK–B cell interactions and NK cell contact with collagen fibers in four dimensions. All data are representative of three to five independent experiments.

Adhesion Assay. NK cell adhesion to collagen I-coated plates (Sigma–Aldrich, St. Louis, MO) was analyzed by using a standard adhesion assay per the manufacturer's instructions.

Cytotoxicity Assays *in Vitro*. NK cells were either treated with DX5 microbeads, DX5-biotin Ab, or DX5-biotin Ab plus streptavidin or they were left untreated before culturing in IL-2-supplemented media (RPMI medium 1640 with 10% FCS, L-glutamine, 50 μM β-ME, and 4,000 units/ml human rIL-2). After 2 days, NK cells were harvested and titrated concentrations were cocultured in V-bottom 96-well plates at 37°C with 1×10^5 0.2 μM CFSE-labeled ($CFSE^{lo}$) YAC-1 target cells per well. After 6 h, cells were stained with propidium iodide for 10 min, washed, and 1×10^5 2 μM CFSE-labeled ($CFSE^{hi}$) target cells were added to each well. Viable cells (FS/SS and propidium $iodide^-$ gates) were analyzed by FACS.

Cytotoxicity Assays *in Vivo*. $B220^+$ B cells from C57BL/6 and BALB/c mice were labeled with 0.2 μM (C57BL/6) or 2 μM (BALB/c) CFSE, and equal numbers (5 to 10×10^6) of cells were coinjected i.v. into C57BL/6 mice (WT), $\gamma c^{-/-}$ mice (KO), and KO recipients reconstituted 1 day prior with either 1 to 1.5×10^7 DX5 microbead-treated or untreated NK cells. Spleens were harvested 12 to 16 h later and analyzed by FACS.

Percent rejection was calculated as follows: 100 (1 − number of $CFSE^{lo}$ events ÷ number of $CFSE^{hi}$ events), where 12,000 $CFSE^{hi}$ events were counted in each condition.

Statistics. Statistical significance was determined by using Student's t test, and $P < 0.05$ was considered significant. Data are presented as mean ± SEM.

We thank Lu Forrest for outstanding veterinary support and guidance on animal handling, and George Chandy and Marian Waterman for helpful comments and discussion of the manuscript. This work was supported by National Institutes of Health Grants GM-41514 (to M.D.C.) and GM-48071 (to I.P.).

1. Lanier LL (1998) *Annu Rev Immunol* 16:359–393.
2. Lanier LL (2005) *Annu Rev Immunol* 23:225–274.
3. Yu G, Xu X, Vu MD, Kilpatrick ED, Li XC (2006) *J Exp Med* 203:1851–1858.
4. Martin-Fontecha A, Thomsen LL, Brett S, Gerard C, Lipp M, Lanzavecchia A, Sallusto F (2004) *Nat Immunol* 5:1260–1265.
5. Chen S, Kawashima H, Lowe JB, Lanier LL, Fukuda M (2005) *J Exp Med* 202:1679–1689.
6. Miller MJ, Wei SH, Parker I, Cahalan MD (2002) *Science* 296:1869–1873.
7. Halin C, Rodrigo Mora J, Sumen C, von Andrian UH (2005) *Annu Rev Cell Dev Biol* 21:581–603.
8. Bajenoff M, Breart B, Huang AY, Qi H, Cazareth J, Braud VM, Germain RN, Glaichenhaus N (2006) *J Exp Med* 203:619–631.
9. Arase H, Saito T, Phillips JH, Lanier LL (2001) *J Immunol* 167:1141–1144.
10. Schwartz MA, Schaller MD, Ginsberg MH (1995) *Annu Rev Cell Dev Biol* 11:549–599.
11. Juliano RL, Haskill S (1993) *J Cell Biol* 120:577–585.
12. Mainiero F, Gismondi A, Soriani A, Cippitelli M, Palmieri G, Jacobelli J, Piccoli M, Frati L, Santoni A (1998) *J Exp Med* 188:1267–1275.
13. Mombaerts P, Iacomini J, Johnson RS, Herrup K, Tonegawa S, Papaioannou VE (1992) *Cell* 68:869–877.
14. Schuster DP, Kovacs A, Garbow J, Piwnica-Worms D (2004) *Am J Respir cell Mol Biol* 30:129–138.
15. Lappin MB, Weiss JM, Delattre V, Mai B, Dittmar H, Maier C, Manke K, Grabbe S, Martin S, Simon JC (1999) *Immunology* 98:181–188.
16. Ferlazzo G, Pack M, Thomas D, Paludan C, Schmid D, Strowig T, Bougras G, Muller WA, Moretta L, Munz C (2004) *Proc Natl Acad Sci USA* 101:16606–16611.
17. Mempel TR, Pittet MJ, Khazaie K, Weninger W, Weissleder R, von Boehmer H, von Andrian UH (2006) *Immunity* 25:129–141.
18. Alter G, Malenfant JM, Altfeld M (2004) *J Immunol Methods* 294:15–22.
19. Shimaoka M, Takagi J, Springer TA (2002) *Annu Rev Biophys Biomol Struct* 31:485–516.
20. Miyake S, Sakurai T, Okumura K, Yagita H (1994) *Eur J Immunol* 24:2000–2005.
21. Street SE, Hayakawa Y, Zhan Y, Lew AM, MacGregor D, Jamieson AM, Diefenbach A, Yagita H, Godfrey DI, Smyth MJ (2004) *J Exp Med* 199:879–884.
22. Bousso P, Robey E (2003) *Nat Immunol* 4:579–585.
23. Okada T, Miller MJ, Parker I, Krummel MF, Neighbors M, Hartley SB, O'Garra A, Cahalan MD, Cyster JG (2005) *PLoS Biol* 3:1047–1061.
24. Fanning SL, George TC, Feng D, Feldman SB, Megjugorac NJ, Izaguirre AG, Fitzgerald-Bocarsly P (2006) *J Immunol* 177:5829–5839.
25. Freud AG, Becknell B, Roychowdhury S, Mao HC, Ferketich AK, Nuovo GJ, Hughes TL, Marburger TB, Sung J, Baiocchi RA, *et al*. (2005) *Immunity* 22:295–304.
26. Gilhar A, Ullmann Y, Kerner H, Assy B, Shalaginov R, Serafimovich S, Kalish RS (2002) *J Invest Dermatol* 119:384–391.
27. Ottaviani C, Nasorri F, Bedini C, de Pita O, Girolomoni G, Cavani A (2006) *Eur J Immunol* 36:118–128.
28. Ferlazzo G, Tsang ML, Moretta L, Melioli G, Steinman RM, Munz C (2002) *J Exp Med* 195:343–351.
29. Fernandez NC, Lozier A, Flament C, Ricciardi-Castagnoli P, Bellet D, Suter M, Perricaudet M, Tursz T, Maraskovsky E, Zitvogel L (1999) *Nat Med* 5:405–411.
30. Gerosa F, Baldani-Guerra B, Nisii C, Marchesini V, Carra G, Trinchieri G (2002) *J Exp Med* 195:327–333.